MECHANICS METHODOLOGY FOR TEXTILE PREFORM COMPOSITE MATERIALS

Clarence C. Poe, Jr.
M.S. 188E
NASA Langley Research Center
Hampton, VA 23681-0001

ABSTRACT

NASA and its contractors have completed a program to develop a basic mechanics underpinning for textile composites. Three major deliverables were produced by the program:

1. a set of test methods for measuring material properties and design allowables
2. mechanics models to predict the effects of the fiber preform architecture and constituent properties on engineering moduli, strength, damage resistance, and fatigue life
3. an electronic data base of coupon type test data

This report describes these three deliverables.

KEY WORDS: Textile Composites, Mechanical Properties, Test Methods, Analysis, Data Base

1. INTRODUCTION

NASA and its contractors have completed Phases A and B of the Advanced Composites Technology (ACT) program to develop composite wings and fuselages for a commercial transport airplane with costs that are competitive with those of current metal airplanes. Textile composites were considered for many components to improve structural performance and to reduce costs. Boeing developed advanced composites for making large crown, side, and keel panels for a fuselage, Lockheed-Martin teamed with Boeing to evaluate textile composites for fuselage frames, window-belt reinforcements, and various components in the keel of the fuselage. Northrup Grumman evaluated textiles concepts for making stiffened skins using 3-D textile composites, and McDonnell Douglas evaluated knitted/stitched textile fabrics for a wing box. To support these activities, a NASA Langley in-house team planned and implemented a program to develop a basic mechanics underpinning for the textile composites. Summaries of that work were published in (1).

The geometry of periodic textiles can be described by spatially translating copies of unit cells, without rotations or reflections. The unit cells of braids and weaves can be 2 to 20 mm in length and width and up to the thickness in depth. On the other hand, the length and width of a unit cell of a laminate made from prepreg tape is on the order of a fiber diameter, 5 to 8 microns. Thus, the inplane displacement fields of a textile composite will be macroscopically inhomogeneous compared to a tape laminate. The field of inplane normal displacements in the loading direction of a tension coupon is shown in Figure 1 for a triaxial braid (2). In a triaxial braid, the braider yarns arebraided about the fixed yarns, which are relatively straight. The fixed yarns in Figure 1 are perpendicular to the loading direction. For uniform displacements (constant strain), the wavy lines (fringes) would be straight and equally spaced. The locations of the yarns are evident in the waviness of the fringe patterns. The braider yarns are associated with the joggles in the fringes, which are caused by large, intense shearing between the yarns in regions of high resin content. The rotations (shearing) reverse where the braider yarns cross one another on the surface. Normal strain varies inversely with line spacing. Thus, the normal strains are highest over the fixed yarns and lowest where the braider yarns cross. The average strains in these two regions differ by a factor of three. The inhomogeneity in Figure 1 raised concerns about strain measurements on test specimens and about adequate specimen size to measure bulk or average mechanical properties and to understand notched strength and damage tolerance behavior of textile composites. This large level of inhomogeneity guided planning of the program to develop a basic mechanics underpinning for the textile composites.

The participants in the Mechanics of Textile Composites Program included aerospace companies, universities, and NASA. A review of this program with technical highlights is given in (3). The program had three primary objectives. First, test methods were developed or modified to establish a set of test methods for measuring material properties and design allowables. Second, mechanics models were developed to predict the effects of the fiber preform architecture and constituent properties on engineering moduli, strength, damage resistance, and fatigue life. Third, coupon-type test data that were generated on textile composites in the ACT program was compiled into an electronic data base.

The program objectives have been largely accomplished, and the results integrated together into engineering guidelines for mechanics of textile composites, which contain the essential engineering methodology required to design airframe-type structural components using textile preform composites. These guidelines are contained in three NASA reports: Standard Test Methods For Textile Composites (4), Handbook of Analytical Methods for Textile Composites (5), and Database of Mechanical Properties for Textile Composites (6). These reports are also available in electronic format from the Langley Technical Report Server (LTRS) using the Uniform Resource Locator (URL): http://techreports.larc.nasa.gov/ltrs. This paper summarizes the contents of these three reports.

Several out-of-plane and impact test methods were not sufficiently mature to be included in (4). Thus, a review of that work is included in this paper for completeness. Another important investigation that should not be overlooked is an experimental comparison of mechanical propertes of 2-D triaxial braids and equivalent prepreg tape laminates (7).

2. STANDARD TEST METHODS FOR TEXTILE COMPOSITES

Strain gages are commonly applied to composite coupons to obtain a stress-strain curve, to measure elastic constants, and to check alignment of test coupons. Strain

gages are also applied to structural components to make strain surveys. The inhomogenious field of displacements in Figure 1 for a triaxial braid suggests that strains should be averaged over several unit cells. Thus, a study was made to determine appropriate strain gage size for textile composites (2). When strain gages were longer than the unit cell, the coefficient of variation in modulus was less than five percent and strain gages and extensometers were in good agreement.

2.1 Test Methods Evaluated by Lockheed Engineering & Sciences Co. Aerospace companies have developed test methods to derive design allowables for laminated prepreg tape composites. This work is ongoing in organizations such as American Society for Testing Materials (ASTM), MIL-HDBK-17, and Suppliers of Advanced Composites Materials Association (SACMA). Because many test methods used by industry are not formal standards, a survey was made of aerospace companies to determine the test methods used most commonly to derive design allowables for laminated prepreg tape composites. These companies have significant experience designing and manufacturing structures made of high-performance composite materials. The objective of the survey was to determine the minimum test methods that should be evaluated for textile composites. Table 1 lists the different types of test methods that were compiled from the survey.

The Boeing Defense & Space Group made textile composites and conducted experiments to evaluate the test methods in Table 1. The results were reported in (8). The textile composites were made using 2-D triaxially braided fabric, stitched uniweave fabric, and 3-D interlock woven fabric. The fabrics were made of AS4 fiber, and the composites were resin-transfer molded using Shell 1895 epoxy. In addition, Lockheed-Martin conducted similar coupon tests to develop allowables for use in ACT fuselage trade studies, the University of West Virginia conducted open-hole tests on some of the triaxial braids to develop failure models (9), and NASA LaRC conducted four-point bend tests on the braids and weaves to develop an improved method to measure out-of-plane tension strengths (10). Lockheed Engineering & Sciences Co. evaluated all these results to determine the best of the test methods in Table 1 (11-15). Criteria such as low coefficient of variability, appropriate failure mode, and simplicity were used. Those selections, which are listed in the right-hand column of Table 1, are reported in (4).

None of the inplane shear test methods were totally acceptable. The methods gave reasonably similar values of shear modulus for a given material, but the coefficients of variation were high for some materials. The coefficients of variation were even larger for strength. Surprisingly, the coefficients of variation for tubes typically were larger than those for the rail shear and compact specimens. Of course the manufacturing methods for the tubes were also significantly different from those of the flat plates. Thus, some of the variability in the tube data may have resulted from the manufacturing method. In some of the rail shear specimens, bearing failures occurred where the rails are bolted to the specimen. The compact specimen, which was clearly the cheapest and most simple to test and gave relatively low coefficients of variation, was generally the best of the group. Because of variations between manufacturing methods for plate and tubes, the tube should probably be tested for tubular applications. Additional work is necessary to develop a shear test method.

Several bend specimens and test methods were evaluated for determining interlaminar tension strength. Boeing evaluated C- and L-Shaped Bend specimens (8) and NASA LaRC evaluated the Four-Point-Bend Specimen (10). The four-point-bend test method was recommended because of the simplicity associated with a section of constant bending moment. Values of interlaminar tension strength were calculated using the same expressions as those used for tape laminates. The four-point-bend test method produced interlaminar failures in the 2-D braids and in plain and 5-

harness-satin 2-D weaves. However, the four-point-bend test method did not produce interlaminar failures in the 3-D weaves. Instead, premature failures resulted from radial matrix cracks associated with the bending.

The relationship between unnotched tension strength and specimen size was investigated for the unnotched tension specimens made of the triaxial braid. For specimen widths between 25 and 63 mm (1.2 and 6.0 times the unit cell widths), mean strengths and coefficients of variation exhibited little correlation with specimen width. (Specimen lengths varied from 16.9 to 54.6 times the unit cell lengths.) Also, strengths of 3.2- and 6.3-mm thick specimens were within 10% of one another.

2.2 Other Interlaminar Test Methods Interlaminar test methods are desirable for optimizing the type and amount of through-the-thickness reinforcement in textile composites. For a constant fiber volume fracture, an increase in through-the-thickness reinforcement results in a decrease in inplane reinforcement and consequently a decrease in inplane stiffness and strength. The interlaminar test methods in Table 2 were evaluated. Although these test methods were not sufficiently mature to be included in the report on Standard Test Methods For Textile Composites, a review of that work is included in this paper for completeness.

2.2.1 Interlaminar Fracture Toughness Boeing conducted Double Cantilever Beam (DCB) and End Notch Flexure (ENF) tests on four of the 2-D triaxial braids to measure Mode I (G_I) and Mode II (G_{II}) interlaminar fracture toughness, respectively (8). 2-D braids are quasi-laminar in nature. The values of G_{II} where two to three times those of G_I, and both G_I and G_{II} were considerably greater than those for prepreg tape laminates. Coefficients of variation, which were 13 to 40%, were also greater than those for prepreg tape laminates.

University of Florida conducted DCB and ENF tests on stitched uniweave composites to measure G_I and G_{II} (16). The specimens were unidirectional except for a layer of fiberglass cloth on each surface to prevent the stitches from pulling through. Values of G_I and G_{II} were much greater than those of unstitched specimens. Because of crack bridging, G_I and G_{II} increased with crack length, especially for G_{II} where the crack front propagated without breaking any stitches. Thus, the toughness values do not represent a material property.

2.2.2 Interlaminar Tension Two types of flat-wise tension test methods were evaluated by University of Delaware for 3-D weaves - a bi-material specimen and a specimen with surface pile (17). Special 25-mm-thick versions of the 3-D weaves were used. Tension load was applied to the bi-material specimen by gripping long metal beams that were bonded to each face of the composite and were bonded to the surface pile of the other specimen by gripping a composite made of the pile yarn. Because failures occurred at the interface, neither specimen was suitable for measuring tension strength. However, both methods were suitable for obtaining interlaminar elastic constants.

2.2.3 Interlaminar Compression An IITRI specimen configuration was evaluated by University of Delaware (17). The same 25-mm-thick 3-D weaves were used as those used for the bi-material tension specimen. The specimen also resembled the bi-material tension specimen except that the metal beams were replaced by Glass/epoxy beams to produce a more uniform stress state. The specimen dimensions were chosen to minimize the stress singularity at the corners of the bond interface. Elastic constants and strengths were reasonable. Failure appeared to be associated with shear damage in the warp and weft tows rather than shear kinking of the weaver tows. Again, the lower limit of thickness for this specimen was not evaluated.

2.2.4 Interlaminar Shear Compact and double-notch (ASTM D-3846) shear specimens were evaluated by University of Delaware (17). Dimensions of both were modified to test the same 25-mm-thick 3-D weaves as those tested with the bi-material tension specimen. Also, the ASTM D-3846 double-notch shear specimen was used to test the 6-mm-thick 3-D weaves. The weaves were tested with two orthogonal directions to obtain τ_{23} and τ_{32} properties, where directions 1, 2, and 3 are associated with warp, weft, and thickness directions. Shear moduli were obtained satisfactorily in all cases, but not strengths. Strengths τ_{32} were obtained satisfactorily for the 25-mm-thick weaves using the modified compact specimen and for the 6-mm-thick weaves using the modified double-notch shear specimen. These strengths were also in good agreement for the two thicknesses. However, strengths τ_{23} were not obtained satisfactorily; the modified compact and double-notch specimens failed outside the test section. Although the modified compact specimen is less complex than the double-notch specimen, it cannot be used for thin composites.

Boeing also evaluated the Short Beam Shear (SBS) and Compression Interlaminar Shear (CIS) Specimens (8). The CIS specimen is similar to the Double-Notch Shear Specimen evaluated by University of Delaware. (For the SBS specimens, the load is applied transverse to the plane of the plate; but for the CIS specimens, the load is applied parallel to the plane of the plate.) The 2-D braids and 3-D weaves were tested. Interlaminar shear strengths by SBS were 20% greater than those by CIS on average. Also, coefficients of variation were lower for SBS than for CIS. Strengths were similar for the 2-D braids and 3-D weaves. (The median value was 43 MPa.)

2.3 Impact The work on impact test methods is not sufficiently mature to be included in the report on Standard Test Methods For Textile Composites. Although additional work is needed, a review of the work is included here for completeness.

2.3.1 Quasi-Static Impact Behavior First, a discussion of quasi-static impact behavior will be useful. Assuming that the force-displacement relationship for a falling weight impact test is the same as that of a quasi-statically loaded plate (quasi-static behavior), the following "energy balance" equation can be derived (18).

$$\frac{1}{2} m_i v_i^2 = \frac{1}{2} \frac{F_{max}^2}{k} + \frac{2}{5} \frac{F_{max}^{5/3}}{n_o^{2/3} R_i^{1/3}} \qquad [1]$$

F_{max} is the impact force, m_i is the mass of the impacter, v_i is the velocity of the impacter, R_i is the radius of the spherical impacter, and k is the flexural stiffness of the plate for a quasi-statically applied impact force. The term on the left hand side of equation 1 is the kinetic energy of the impacter, and the first and second terms on the right hand side of equation 1 account for flexural displacements and for Hertzian indentation, respectively. For thin plates, the Hertzian term is negligible, and impact force increases in proportion to the square root of the product of kinetic energy and flexural stiffness.

Dynamic finite element analyses were made of 7.0-mm-thick AS4/3501-6 $[45/0/-45/90]_{6S}$ plates impacted with various masses having a 12.7-mm-diameter tup (18). Viscoelastic effects and damage were not taken into account. In Figure 2, the maximum calculated values of impact force are plotted against the frequency ratio $\omega^2/(k/m_i)$ for a constant value of impacter kinetic energy, where w is the natural frequency of the plate and $(k/m_i)^{1/2}$ is a pseudo natural frequency of the impacter mass and plate. For homogeneous uniformly thick plates, $\omega^2/(k/m_i) = (m_i/m_p)/\alpha^2$,

where α = 0.471 and 0.371 for simply supported and clamped boundaries, respectively. Results are plotted for three square plates with various sizes and boundary conditions. In general, impact force decreases with increasing impacter mass and plate size and is less for simply supported than clamped boundary conditions.

The time of contact from the dynamic finite element analyses decreased with decreasing impacter mass. Thus, the number of reflections from the boundaries before the impact force reached a peak decreased with decreasing impacter mass. When impacter mass was to the left of the vertical dashed lines in Figure 2, no reflections returned before the impact force reached a peak, and impact force was not affected by plate size nor boundary conditions. The horizontal dashed lines in Figure 2 represent calculations with equation 1 and n_o = 4.52 GPa. For large values of impacter mass, the dynamic analysis curves asymptotically approach equation 1 as the number of reflections become large, indicating that the force-displacement relationships are quasi-static.

2.3.2 Impact Test Methods In Current Use The NASA and SACMA impact test methods in Table 3 are the most commonly used for falling weight impact tests. For specimens 6-mm-thick or less, which is usually the case, $(m_i/m_p)/\alpha^2 > 70$ for the specimen sizes and impacter masses in Table 3. Thus, the analytical results in Figure 2 indicate that impacts are essentially quasi-static for both methods.

It is useful to think of impact response as having two aspects: damage resistance (size of damage for a given impact force) and damage tolerance (strength for a given size of damage). Neither of the test methods in Table 3 specifies the measurement of impact force, but impact force can be measured in a falling weight test with an instrumented tup. With measurements of impact force, both damage resistance and damage tolerance can be determined; without impact force, only damage tolerance can be determined.

2.3.3 Recommended Damage Resistance Test Method Metrics for damage resistance were developed in (18). Damage diameters from C-scans are plotted against impact force in Figure 3 for laminates made of AS4/3501-6 and IM7/8551-7 prepreg tape. The 3501-6 is a brittle epoxy, and the 8551-7 is a toughened epoxy. Data are plotted for both quasi-static indentation (QSI) and falling weight impact tests. The QSI tests were conducted by mounting an instrumented tup with 12.7-mm diameter in a universal testing machine and forcing the indenter against a specimen clamped over a 10.2-cm-diameter circular opening. For the falling weight tests, the same tup was used and the specimens were clamped over a 12.7-cm-square opening. The damage initiated when a critical value of impact force F_1 was exceeded; then the damage diameter increased in proportion to impact force. (The diameter was calculated for a circle equal in area to the C-scan image.) The change in damage diameter with impact force was inversely proportional to a transverse shear strength per unit length Q*. Damage from the QSI tests and falling weight tests were approximately the same size for a given impact or contact force. (Other investigations have shown similar results.) The values of Q* and F_1 for IM7/8551-7 are significantly greater than those for AS4/3501-6. Values of Q* and F_1 were also found to increase significantly with increasing thickness (10). Both Q* and F_1 can be used as metrics for damage resistance.

Values of Q* and force F_1 for the 2-D braids and 3-D weaves and for stitched uniweave composites supplied by McDonnell Douglas are given in (10). The stitched uniweave materials are described in (19).

Both falling weight and QSI tests can be used to measure damage resistance. However, QSI tests have the following advantages:

1. The test can be conducted using a universal testing machine, which is available in most laboratories and can readily measure contact force.
2. Contact force can be readily controlled, giving more direct control over damage.
3. Damage tolerance criteria tend to be based on a visibility metric such as dent depth rather than impacter kinetic energy. (The force-displacement relationship can be integrated to give a reasonably accurate estimate of impacter energy under quasi-static conditions. Thus, impact energy levels to produce specific levels of damage can be determined efficiently.)

A subcommittee of ASTM committee D30 on composites is in the final stages of developing a standard QSI test method.

The ASTM QSI method and a modified NASA method are recommended in Table 4 for measuring damage resistance. (The weak clamping apparatus and the 32-mm-thick plywood baseplate of the SACMA method may result in impact forces and consequently damage sizes that are less than those for the NASA method.) A circular opening is recommended to give polar symmetry for the apparatus. The specimens should be securely clamped over the opening, and the diameter of the opening should be greater than the diameter of the damage. (No significant difference was found in (20) among values of Q^* in QSI tests with fixture opening diameters varying between 5.1 cm and 10 cm and with damage diameters ranging between 30 and 60% of fixture opening diameters.) The MIL-STD-1530A specifies a 25.4-mm-diameter impacter. (Larger diameter tups have been shown to give larger nonvisible damage (21).) Thus, the standard tup diameter should be increased to 25.4 mm. Of course, other tup diameters could be used as necessary. For the modified NASA method, the tup should be instrumented to measure impact force. (An instrumented tup can also be used for the QSI test if the load cell of the testing machine is too large to give accurate readings.) To assure quasi-static behavior for the modified NASA method, the impacter mass should be at least 10 times that of the specimen (based on the unsupported size of the specimen). The reader should be aware that the impact forces in Figure 2 are sometimes smaller for the quasi-static situation than for small masses. Thus, damage may be smaller for the quasi-static situation than for small masses.

2.3.4 Recommended Test Method For Measuring Damage Tolerance A modified NASA method is recommended in Table 5 for measuring post-impact tension and compression strength (damage tolerance). The recommended specimen width is at least 3 times the damage diameter, and the length is two times the width plus additional length for introducing load. The compression method uses the NASA type of edge and end supports to prevent Euler buckling. The tension method does not require edge or end supports; the length l will be determined by the load introduction method.

The specimen width in Table 5 was chosen using the following analysis. The material damaged by impact carries much less load than the undamaged material, and can be conservatively represented as an open hole of equal diameter. The stress at the edge of an open hole in an isotropic sheet of finite width was normalized by three times the far-field stress and plotted against ratio of hole diameter to sheet width in Figure 4 (22). A ratio of hole diameter to specimen width of 0.3 would result in a stress ratio of only 1.12. Thus, one would expect the far-field stress at failure for an infinite specimen to be no more than 112% of a specimen with a ratio of hole diameter to specimen width of 0.3. For a 2.5-mm dent (MIL-STD-1530A), the damage diameter for a 6-mm-thick specimen was 7 cm (23), which is 54% and 70% of the specimen widths in Table 3. For a 7-cm-diameter hole and the specimen widths in Table 3, the

stress ratios in Figure 4 are 1.55 and 2.30. Thus, post-impact strengths would likely be extremely conservative.

3. HANDBOOK OF ANALYTICAL METHODS FOR TEXTILE COMPOSITES

The report on Handbook of Analytical Methods for Textile Composites includes sections on

- Overview of textiles
- Choice between textiles and tape laminates
- Failure mechanisms
- Predicting elastic constants and thermal expansion
- Nonlinear stress-strain behavior and strength
- Fatigue life
- Summary of available computer codes

A bibliography is also included. A brief overview of these sections follows.

3.1 Overview of Textiles Textiles were categorized by their two and three dimensional fiber architecture and by their quasi-laminar and nonlaminar characteristics. Processes were described for weaving, braiding, knitting, and stitching fiber preforms and for infiltrating the preforms with resin and for molding to net shape. Powder coating and commingling methods were also described for combining resin and fiber prior to and during the textile process.

Ideal unit cell geometries were described for various textile processes. Equations were given that relate fiber volume fraction and textile geometry in terms of process parameters. Irregularities in ideal geometry were described. Examples were given of integral structure made by textile processes.

3.2 Choice between Textiles and Tape Laminates Textiles and tape laminates were contrasted with regard to handling, manufacturability, and mechanical properties. Dry textile preforms can be handled in net form, stored indefinitely, and draped over and into forms of complex curvature. However, the final fiber architecture can be disturbed significantly by handling and draping. Stiffness and unnotched strength of textiles tend to be less than those of tape laminates because of the yarn crimp introduced by interlacing in the textile process - strength more than stiffness. On the other hand, notched strengths of textiles and tape laminates can be nearly equal for equivalent areal weights of fiber. For 3-D (nonlaminar) type textiles, delaminations and failures associated with secondary bonds can be reduced or eliminated. The size of impact damage can be greatly reduced by stitching.

3.3 Failure Mechanisms Failure mechanisms for nominal shear, compression, and tension were discussed. In shear and tension, failure typically begins in the resin where shear and tension stresses are large, much as in tape laminates. But failures tend to occur at lower nominal strains in textiles than tapes because yarns of textiles are much larger than plies of tape. Delaminations and kink bands can form in textiles much as in tape laminates. However, delaminations are not likely to form in the nonlaminar textiles. Even in quasi-laminar textiles, crimp in yarns almost assures kink band formation.

In both tension and compression, nonlinear processes at the notch ameliorate the local stresses and make textiles remarkably notch insensitive. The large yarns enhance the nonlinear processes. Preliminary experiments did not reveal any alarming degradation of strength due to fatigue. Damage developed more quickly in compression fatigue than in tension fatigue, much as in tape laminates. The failure mechanisms in monotonic and fatigue loading were similar.

3.4 Predicting Elastic Constants and Thermal Expansion Mathematical modeling concepts were reviewed. Isostrain and isostress assumptions were contrasted. Tows are typically assumed to be homogeneous and transversely isotropic. Because tows are more tightly compacted than tape laminates, elastic constants of tapes cannot be used. Thus, micromechanics theories are used to calculate elastic constants for the tows. (Fiber volume fractions for tape laminates are typically 0.6. Even though fiber volume fractions for textiles composites are typically 0.5 to 0.6, the fiber volume fraction in the individual tows may exceed 0.7.)

Analyses are usually made of representative volumes of textiles called unit cells. Unit cells, appropriate boundary conditions, and length scales for macroscopic behavior were discussed. Equations for average strain, stress, and virtual work theorems were derived. Also, equivalent stiffness and compliance matrices were derived by orientation averaging.

The capabilities of computer codes listed in Table 6 were reviewed. The mechanics assumptions and methods used to represent textile geometry were described for each code. Applications of the codes to quasi-laminar textiles was discussed.

Plate stiffnesses (A, B, and D matrices of Classical Lamination Theory (CLT)) and elastic constants were calculated for a carbon/epoxy plain weave. Experimental values and calculations by CLT and a finite element method (FEM) were compared. The CLT calculations were made for a laminate with equivalent areal weights of fiber and equal overall fiber volume fraction. Some of the values of plate stiffness did not agree well. The differences were attributed to the manner in which bending-stretching coupling was taken into account. These differences should diminish with increasing number of layers. Except for ν_{12}, the elastic constants were in general agreement for the various codes and experiments. The value of ν_{12} calculated using μTex-10 was in agreement with the test value, but the other calculated values were about one third of the test value.

3.5 Nonlinear Stress-Strain Behavior and Strength Matrix plasticity, matrix cracking, and rotations of crimped tows (straightening) typically preceded catastrophic failure of the tows. This progression of damage results in nonlinear stress-strain behavior. The capabilities of the computer codes to predict local stresses, nonlinear stress-strain behavior, and strength are given in Table 6. None of the models can analyze notched textile composites.

3.6 Fatigue Life A kink band formation model for compression fatigue was reviewed. The stress to cause kink band formation is given by

$$\sigma_k = \tau_c / \phi \qquad [2]$$

where τ_c is the flow stress and ϕ is the misalignment angle. Values of ϕ were determined by examining photomicrographs of the textile composite. The flow stress was assumed to deteriorate with cycles of load according to

$$\frac{d\tau_c}{dN} = -A(\Delta\sigma_s\phi)^m \qquad [3]$$

where $\Delta\sigma_s$ is the cyclic stress amplitude and A and m are material constants. Integrating equation 4,

$$N_k = \frac{\tau_c - \Delta\sigma_s\phi}{A(\Delta\sigma_s\phi)^m} + 1 \qquad [4]$$

For load controlled fatigue tests, fatigue failures followed formation of just a few kink bands. Values of m were 30 for carbon/epoxy 3-D interlock weaves and 15 for glass/urethane 2-D triaxial braids. For strain controlled fatigue tests of carbon/epoxy 3-D interlock weaves, fatigue failure did not follow formation of a few kink bands. Instead, the number of kink bands increased gradually.

3.7 Summary of Available Computer Codes A summary and user's guides of the computer codes in Table 6 was provided. The authors names, references, modeling assumptions, source code language, and description of input and output are given.

4. A DATABASE OF MECHANICAL PROPERTIES FOR TEXTILE COMPOSITES

The test data was assembled from the NASA Advanced Composite Technology (ACT) program and from the public domain. The data documentation requirements of MIL-HDBK-17, Section 8.1.2 were satisfied. Properties were included for

- 2-D triaxial braids
- 3-D multiaxial braids
- stitched uniweaves
- 8 harness weaves
- 3-D interlock weaves
- stitched multiaxial warp knits
- uniweaves

Materials and product forms are given in Table 7. Each material and product form is characterized by a set of textile parameters. For example, braids are characterized by axial and braider tow sizes and spacings, by braid angle, etc.

The database include the following elastic properties and strengths:

- Tension and compression moduli
- Shear moduli
- Poisson's ratios
- Unnotched tension and compression strengths
- Open-hole tension and compression strengths
- Filled-hole tension and compression strengths

- Bearing
- Through-the-thickness tension
- Tension and compression after impact
- Inplane shear
- Fatigue
- Biaxial tension and compression

Not all elastic properties and strengths were available for all material subclasses and product forms.

MSC/MVISION, which requires a work station with a UNIX operating system, was chosen for the principal database manager. The schema hierarchy structure for the MSC/MVISION database is as follows:

Class (material class, schema level...)
Material (material name, material form...)
Constituent (fiber/matrix class, fiber size...)
Preform (textiles preform architecture, preform descriptions...)
Process (process method, tackifier information...)
Molding (panel layup, NDE method...)
Test (test type, test facility, test fixture...)
Coupon (nominal coupon geometry)
Conditioning (test environment, coupon conditioning...)
Actuals (failure loads/stresses, measured values...)

The MSC/MVISION database, which is of moderate size (≈17 megabytes), has two useful features. First, using the **Query panel**, information to be displayed can be limited to specific materials or properties, for example only stitched AS4/RSL-1895 material. Second, values of specific attributes can be selected using the **Select** command. Data for multiple materials and attributes can be selected using operators like **and** and **or**. When multiple tests were conducted, the data for each test is included. Thus, statistical analyses can be performed by the user. Load-deformation curves were included for some tests.

Also, Microsoft Excel was chosen for a summary or executive database manager for PC and Apple Macintosh desktop computers. Much less information about the material, test variables, and test results is given in the Microsoft Excel databases than in the MSC/MVISION database. The Microsoft Excel database has tabs to select specific materials with average properties distributed among the columns.

5. CONCLUDING REMARKS

NASA and its contractors have completed a program to develop a basic mechanics underpinning for textile composites. Three major deliverables were produced by the program:

1. a set of test methods for measuring material properties and design allowables
2. mechanics models to predict the effects of the fiber preform architecture and constituent properties on engineering moduli, strength, damage resistance, and fatigue life
3. an electronic data base of coupon type test data

6. REFERENCES

1. Mechanics of Textile Composites Conference. NASA CP 3311, Parts 1 & 2, Oct. 1995.
2. John E Masters, NASA CR-198286, February 1996.
3. C. C. Poe, Jr. and Charles E. Harris NASA CP-3326, Vol. 1, 1996.
4. John E Masters and Marc A. Portanova, NASA CR-4751, 1996.
5. Brian N. Cox and Gerry Flanagan, NASA CR-4750, 1996.
6. Jerry Delbrey, NASA CR-4747, 1996.
7. Pierre J. Minguet and Christian K. Gunther, NASA CR-4610, July 1994.
8. Pierre J. Minguet , Mark J. Fedro, and Christian K. Gunther, NASA CR-4609, July 1994.
9. Timothy L. Norman, Colin Anglin, David Gaskin, and Mike Patrick, NASA CR-4676, June 1995.
10. Wade C. Jackson and Marc A. Portanova, NASA CP 3311, Part 2, October 1995, pp. 315-348.
11. M. A. Portanova and J. E. Masters, NASA CR-198262, December 1995.
12. M. A. Portanova and J. E. Masters, NASA CR-198263, December 1995.
13. M. A. Portanova, NASA CP-198264, December 1995.
14. M. A. Portanova and J. E. Masters, NASA CP-198266, December 1995.
15. John E. Masters, NASA CP-198285, February 1996.
16. Suresh K. Sharma and Bhavani V. Sankar, NASA CR-195042, February 1995.
17. Dru Hartranft, Azar Pravizi-Majidi, and Tsu-Wei Chou, NASA CP 3311, Part 2, October 1995, pp. 251-314.
18. W. C. Jackson and C. C. Poe, Jr., Journal of Composites Technology & Research, Vol. 15, No. 4, Winter 1993, pp. 282-289.
19. Marc Portanova, NASA CP 3311, Part 2, October 1995, pp. 391-424.
20. Young S. Kwon and Bhavani V. Sankar, NASA CR-187624, March 1992.
21. C. C. Poe, Jr., Proceedings of the American Society for Composites, Third Technical Conference, 1988, pp. 334-343.
22. Raymond J. Rourk, and Warren C. Young, Formulas for Stress and Strain. Fifth Edition. McGraw-Hill Book Co., 1975.
23. M. A. Portanova, NASA CR-198265, December 1995.
24. Peter G. Ifju, NASA CP-3311, Part 1, October 1995, pp. 141-176.
25. NASA Reference Publication 1142, June 1985.
26. SACMA Recommended Test Method for Compression after Impact Properties of Oriented Fiber-Resin Composites, SRM 2-88.

TABLE 1. TEST METHODS EVALUATED AND SELECTED BY LOCKHEED ENGINEERING & SCIENCES CO.

Test method type	Test methods evaluated	Best test methods
Inplane		
Unnotched tension	Straight sided (ASTM D3039) and dog-bone specimens	Straight sided (ASTM D3039) specimens
Unnotched compression	NASA Short Block, Modified IITRI, Boeing OHC, Zabora, Boeing CAI, NASA ST-4, and sandwich column	Zabora
Open-hole tension	Straight sided specimen (ASTM D5766)	Straight sided specimen (ASTM D5766)
Open-hole compression	NASA Short Block, Modified IITRI, Boeing OHC, Zabora, Boeing CAI, NASA ST-4, and sandwich column	Zabora
Filled-hole tension	Straight sided specimen (ASTM D5766)	Straight sided specimen (ASTM D5766)
Bolt bearing	Boeing Unstabilized Single Shear, Boeing Stabilized Single Shear, and Boeing Double Shear	Boeing Stabilized Single Shear
Shear	Tube Torsion, Rail Shear, and Compact Shear (24)	None totally satisfactory
Out-of-plane		
Interlaminar tension	C- and L-Shape Bend and Four Point Bend	Four Point Bend (strength only)

TABLE 2. OTHER OUT-OF-PLANE TEST METHODS EVALUATED

Test method type	Test methods evaluated	Comments
Interlaminar fracture toughness	DCB (Mode I)	Reasonable for 2-D braids and stitched uniweaves
Interlaminar fracture toughness	ENF (Mode II)	Reasonable for 2-D braids
Interlaminar tension	Flat-Wise Tension	Reasonable for elastic constants
Interlaminar compression	Modified IITRI	Reasonable for elastic constants and strength
Interlaminar shear	Compact, Double Notch Shear, and Compression Interlamnar Shear	Compact for thick & Double Notch for thin composites
Interlaminar shear - transverse	Short Beam Shear	Reasonable for 2-D braids and 3-D weaves

TABLE 3. IMPACT TEST METHODS IN CURRENT USE

Test method	Unsup-ported specimen size, cm	Post-impact specimen size, cm	Edge support during impact	Edge support during compres-sion test	[a]Impacter tup diameter, mm	Impacter mass, kg
NASA (25)	13x25	13x25	Clamped	Simply supported	12.7	4.5-5.4
SACMA (26)	7.6x13	10x15	[b] Clamped	Simply supported	15.9	5.0

[a]Hemispherical shaped tups.
[b]The prescribed clamping apparatus more nearly represents simply supported conditions than clamped conditions.

TABLE 4. RECOMMENDED DAMAGE RESISTANCE TEST METHODS

Name	[a]Minimum circular opening dia., cm	Edge support during impact	[b]Impacter tup diameter, mm	[c]Minimum impacter mass, kg
QSI	D	Clamped	25	-
Modified NASA	D	Clamped	25	$2.5\pi\,(\rho h)_p\,xD^2$

[a]D should be larger than the diameter of the impact damage to avoid boundary effects and should be much larger than the specimen thickness to minimize shear deformation effects.
[b]Hemispherical shaped tups.
[c]$(\rho h)_p$ is the product of density and thickness of the specimen.

TABLE 5. RECOMMENDED POST-IMPACT STRENGTH TEST METHOD (DAMAGE TOLERANCE)

Name	[a]Specimen width	[b]Specimen length	Edge support	End support
Compression test				
Modified NASA	$\geq W$	$\geq 2W + \lambda$	[c]Simply supported	Clamped
Tension test				
Modified NASA	$\geq W$	$\geq 2W + \lambda$	None	Clamped in grips or pin loaded

[a]$W = 3d_o$, where d_o is the diameter of the impact damage.
[b] λ represents the additional specimen length required for load introduction.
[c]When appropriate, Euler buckling of large, thin specimens can be prevented by supporting the faces of the specimen.

TABLE 6. SUMMARY OF COMPUTER CODE CAPABILITIES

Code	Textile forms	3-D stiff-ness	Ther-mal expan-sion	Plate stiff-ness	Local stress	Non-linear-ity	Strength
PW	Plain weaves						
SAT5	5 harness satin						
SAT8	8 harness satin		Yes	Yes			
CCM-TEX	3-D weave and 2- and 4-step braids	Yes					Yes
μTex-10	General	Yes	Yes	Yes	Yes		
μTex-20	User defined	Yes	Yes	Yes	Yes		
SAWC	plain weave (FE code)	Yes			Yes	[a]Yes	Yes
TEXCAD	2-D weaves and 2-D braids	Yes	Yes	Yes	Yes	[b]Yes	Yes
WEAVE	3-D weaves	Yes					
BINMOD	3-D weaves	Yes				Yes	Not directly

[a]Stiffness discounting.
[b]Shear hardening and stiffness discounting.

TABLE 7. MATERIAL SUBCLASSES AND PRODUCT FORMS IN DATABASE

Material subclass	Available product forms
AS4/3501-6	Uniweaves, knits, fabric, & tape
AS4/8551-7	Tape
AS4/CET-3	8H satin fabric
AS4/E905-L	3-D braid & 8H satin fabric
AS4/IM7/3501-6	Stitched knit
AS4/PR-500	Braids, weaves, & fabrics
AS4/PT-500	3-D weaves
AS4/RSL-1895	Braids, weaves, uniweaves, & fabrics
AS4/RSS-1952	8H satin fabric
IM7/8551-7	Tape

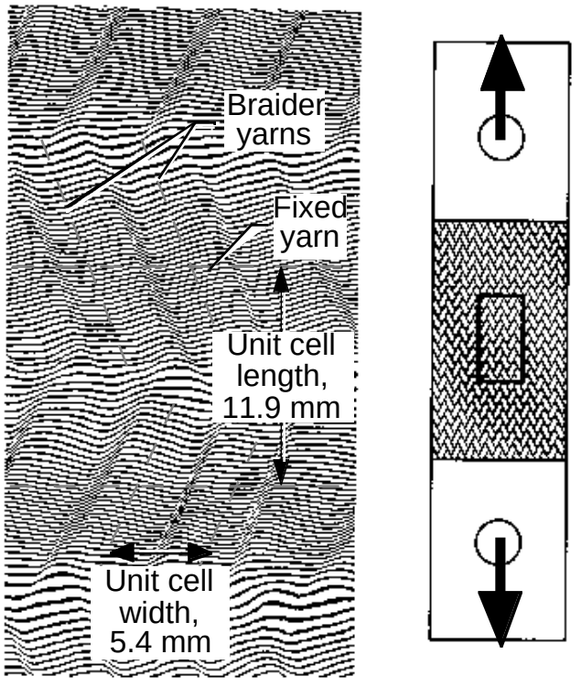

Figure 1. Vertical displacement field in triaxial braid by Moiré.

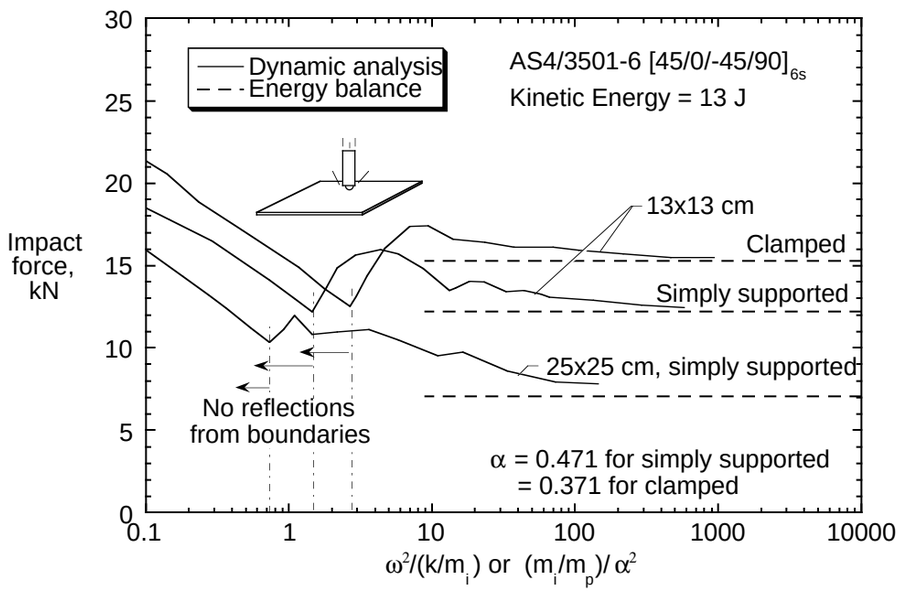

Figure 2. Comparison of dynamic finite element analysis and energy balance equation.

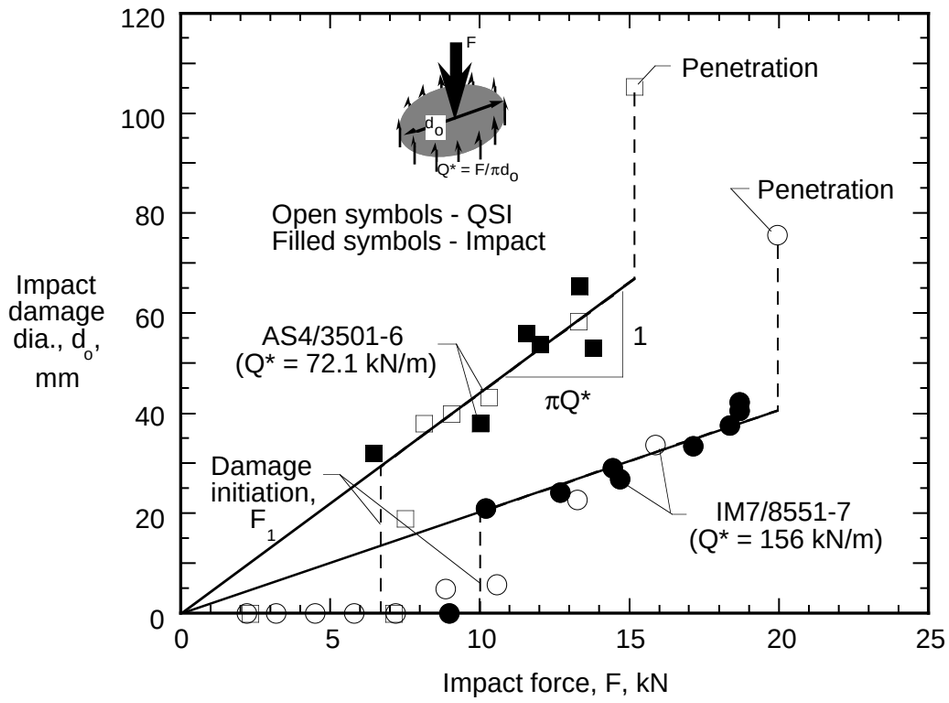

Figure 3. Damage for AS4/3501-6 and IM7/8551-7 $[45/0/-45/90]_{6s}$ prepreg tape laminates (7.1 mm thick) caused by quasi-static indentation and falling weight impact tests.

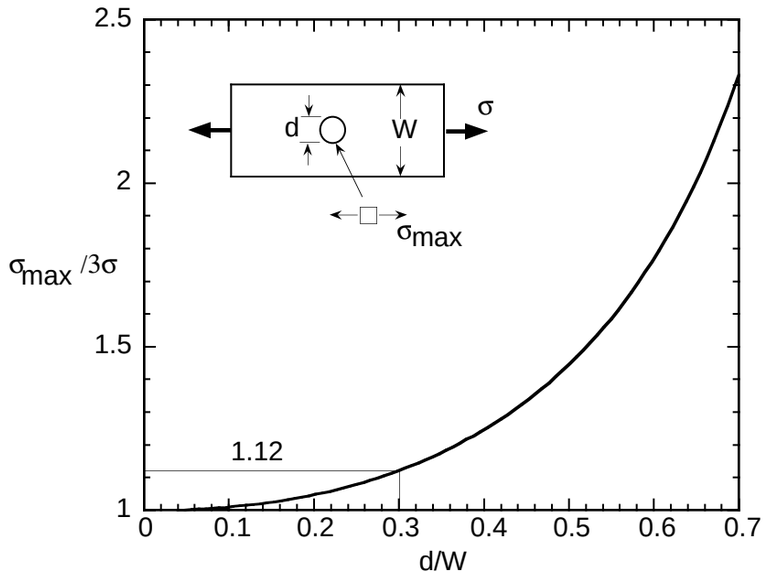

Figure 4. Finite width effect for open hole.